The study of microtubule dynamics and stability at the postsynaptic density in a rat pilocarpine model of temporal lobe epilepsy

Xiaomei Wu[1], Ying Zhou[2], Zhiling Huang[1], Mingfei Cai[1], Yi Shu[1], Chang Zeng[3], Li Feng[4], Bo Xiao[4], Qiong Zhan[1]^

[1]Department of Neurology, The Second Xiangya Hospital, Central South University, Changsha, China; [2]Department of Neurology, The First Hospital of Changsha, Changsha, China; [3]Health Management Center, Xiangya Hospital, Central South University, Changsha, China; [4]Department of Neurology, Xiangya Hospital, Central South University, Changsha, China

Contributions: (I) Conception and design: Q Zhan, B Xiao, Z Huang; (II) Administrative support: Q Zhan, B Xiao; (III) Provision of study materials or patients: X Wu, Y Zhou, L Feng; (IV) Collection and assembly of data: X Wu, Y Zhou, Q Zhan; (V) Data analysis and interpretation: Y Zhou, M Cai, Y Shu, C Zeng; (VI) Manuscript writing: All authors; (VII) Final approval of manuscript: All authors.

Correspondence to: Qiong Zhan. Department of Neurology, The Second Xiangya Hospital, Central South University, Changsha, China.
Email: zhanqiong51@csu.edu.cn.

Background: The recurrence and drug resistance of temporal lobe epilepsy (TLE) has been ceaselessly challenging scientists and epilepsy experts. There has been an accumulation of evidence linking the dysregulation of postsynaptic proteins etiology and the pathology of epilepsy. For example, NMDA receptors, AMPA receptors, and metabotropic glutamate receptors (mGluRs). Furthermore, our earlier proteomic analysis proved there to be differential expressions of cytoskeletons like microtubules among rat groups. These differential expressions were shown in TLE-spontaneous recurrent seizures (TLE-SRS), TLE without SRS (TLE-NSRS) and control groups. Therefore, we aimed to understand how the microtubule system of the hippocampal postsynaptic density (PSD) regulates the development of TLE.

Methods: In this study, a pilocarpine-induced Sprague-Dawley rat TLE model were used, and Western blot, Nissl staining, and the immunoelectron microscopic method were utilized to determine the dynamic change of microtubules (α- and β-tubulin) in PSD and the extent of hippocampal neuron loss respectively in acute SE, and latent and chronic (spontaneous seizures) periods. Animal models were then stereotactically treated using colchicine, a microtubule depolymerizer, and paclitaxel, a microtubule polymerization agent, after each animal's acute SE period so as to further explore the function of PSD microtubules.

Results: Our study revealed 3 principal findings. One, both α- and β-tubulin were decreased from the 3rd to the 30th day (lowest at the 7th day) in the seizure group compared with the controls. Two, both α- and β-tubulin were found to be more downregulated in the TLE-SRS and the TLE-NSRS group than in the control group (especially in the TLE-SRS group). The same trend was also noticed for hippocampal neuron loss. Three, the paclitaxel lowered the chronic SRS rate and increased the expression of PSD β-tubulin in the hippocampus.

Conclusions: Altogether, these results indicate that the microtubule system of PSD may play an essential role in the development and recurrence of epilepsy, and it may be used as a new target for the prevention and treatment of this refractory disease.

Keywords: Colchicine; lithium-pilocarpine rat model; paclitaxel; α-tubulin; β-tubulin

Submitted Dec 30, 2019. Accepted for publication Jun 21, 2020.
doi: 10.21037/atm-19-4636
View this article at: http://dx.doi.org/10.21037/atm-19-4636

^ORCID: 0000-0003-0228-4556.

Introduction

Temporal lobe epilepsy (TLE) is one of the most common and severe types of epilepsy and is well known by its intractable, recurrent, and pharmacoresistant seizures that severely impair the physical and mental health of patients (1). Though there has been considerable progress made in epilepsy research, from the underlying mechanisms to drug and surgery treatment (2), the cause of TLE and the specific neuropathological process remains unclear. Neuroinflammation, neurodegeneration, synaptic reorganization, and rearrangement of excitatory and inhibitory circuitry were reported associating with the occurrence of TLE (3-5). Synapses are the critical structures mediating information transmission between neurons. It has been proven that epilepsy is closely related to the disorders of presynaptic neurotransmitter release, postsynaptic receptor sensitivities, and metabolic status in synaptic space. Since the sensitivity of postsynaptic receptors is the downstream effect of nerve signal transduction that ultimately determines the transmission efficiency of excitatory synapses (6), it may be at the core of the excitatory abnormalities of epileptic neural networks, and thus should to be further explored.

The postsynaptic density (PSD) has been reported to consist of a highly complex proteome which contains about 1,000 conserved proteins which act as sophisticated molecular computational devices (7). The PSD has several proposed functions such as signal amplification, cytoskeletal anchorage, biochemical signaling regulation, and neurotransmitter clustering (8), with its main components consisting of neurotransmitter receptors (especially glutamate and γ-aminobutyric acid receptors), cell scaffold proteins, cytoskeleton, and regulatory proteins. As the molecular composition and structure of PSD can be dynamically regulated by the dendritic spine through mechanisms of protein translation (9), phosphorylation, ubiquitination, and degradation (10-12), leading to enhancement or attenuation of synaptic transmission and change of synapse plasticity, PSD is thought to be an important component for determining synaptic transmission efficiency.

Microtubules (MTs) compose the main cytoskeletal structure of all eukaryotic cells; they consist of α- and β-tubulin heterodimers and are integral in controlling cell shape modification, division, motility, and differentiation (13). MTs can fulfill their specific function through interacting with combined MT-associated proteins (MAPs), which include MAP 1–10, tau, EMLs, GLFND, and dynamism proteins (14). These proteins can regulate MT dynamics by either stabilizing or destabilizing them, generate forces, or connect MTs to other cellular structures, acting as the interface between signaling cascades and MTs (15). Therefore, the stability of MTs is essential for normal cell function, as it is for PSD. Zhang *et al.* found that F-actin, a major cytoskeletal component in the synapses, decreased its expression by 43% in the mossy fiber-CA3 PSD of post status epileptic (SE) mice as compared to controls, indicating a critical long-term effect of SE-involved cytoskeletal modification in this region (16). Some major components of both actin and microtubule cytoskeletons, such as MAP-2 (17) and tau (18,19), were identified as being specifically correlated to network remodeling in hippocampal epilepsy. Our previous PSD proteomic screening study also demonstrated that the cytoskeleton proteins of α- and β-tubulin were downregulated in the TLE-spontaneous seizure group as compared with the non-TLE-spontaneous seizure group and the healthy control group (20). Therefore, we hypothesize that the microtubule system in PSD may play an essential role in the formation of epilepsy.

It is well established that the lithium-pilocarpine induced seizure rodent model is a useful model for human TLE. This model usually develops at the following three stages: primary brain damage (acute period), seizure-free latency (latent period), and spontaneous recurrent seizures (SRS) (chronic period) (21-24). In the present study, we utilized this model to test this hypothesis by examining the dynamic changes of microtubules in PSD and the extent of neuron loss in the hippocampus. From our earlier work, we knew that not all animals would develop to SRS after the latent period. We were also interested in determining whether there was a difference between groups of TLE-SRS and TLE-NSRS (TLE without SRS).

Some interesting effects, such as an anti-seizure phenomenon, have been observed *in vivo* and *in vitro* in several pharmacologically intervened chronic or electrophysiological epilepsy models. These effects were achieved by applying cytoskeletal or microtubule manipulation agents including a tau, a hyper-phosphorylation agent, or nocodazole, a microtubule-stabilizing agent (25-28). As the microtubule fibers are in a state of dynamic assembly and de-assembly, this is referred to as the dynamic instability of the microtubule system, and it is significant for its functions and implementation

(29,30). We additionally used colchicine and paclitaxel, which are classical microtubules depolymerizers (31) and polymerization agents (32), respectively, to interfere with the structure of this microtubule system to see if this intervention could bring a difference to seizure onset after the latent period.

Overall, the aim of the present study was to investigate the role and the potential mechanism of the microtubule dynamics and stability at the PSD in hippocampal neurogenesis in a pilocarpine-induced rat model, and to provide potential new insights into the prevention and treatment of TLE.

We present the following article in accordance with the ARRIVE reporting checklist (available at http://dx.doi.org/10.21037/atm-19-4636).

Methods

Animals

All procedures of this investigations were conducted under approved protocols of Central South University (Changsha, China) Institutional Review Board and were performed in compliance with the National Institutes of Health Guide for the Care and Use of Laboratory Animals (NIH publications, Version 1996) and the ARRIVE Guidelines (33). The study was reviewed and approved by the Animal Ethical and Welfare Committee and the Institutional Animal Care and Use Committee (IACUC), The Second Xiangya Hospital, Central South University, China (Approval No. 2020093).

Healthy, young male and SPF Sprague-Dawley (SD) rats (weighing 250±20 g, aged 6–8 weeks) were used for the study. They were bought from the SLAC Laboratory Animal Co. Ltd (Shanghai, China) and housed in the Experimental Animal Center of Central South University (Changsha, China). All animals were fostered 5 to 6 per cage at a temperature of 22±3 ℃ with humidity of 55%±5% and a regular 12 h light-dark cycle. Water and food were supplied adequately. The number of animals used and their suffering was reduced to a minimum in this work.

Seizure model and groups

The method of modeling was conducted in the same manner as our previous work (34,35). Briefly, the experimental group was treated with lithium chloride (125 mg/kg, i.p., Sigma-Aldrich, USA), and 18–20 h later, methyl atropine bromide (1 mg/kg, i.p. Harvest Pharmaceutical Co. Ltd., China) was used to alleviate the peripheral cholinergic effects and was followed by pilocarpine hydrochloride (20 mg/kg, i.p., Sigma–Aldrich; USA) 30 min later for epilepsy induction. The severity of convulsions triggered was ranked using Racine's classification scale (36). Only those rats showing SE over 50 min and reacing the classification of Racine stage IV–V were used in the present study. Those that did not meet the criteria would receive additional doses of pilocarpine (10 mg/kg; i.p.) every 30 min until they reach the goal or the maximum pilocarpine dose reached 60 mg/kg. Seizures were interrupted with 10% chloral hydrate (3 mg/kg, i.p.) after 50 min of SE. The, animals were monitored 30–60 days for the later latent period (typically 3–14 days after SE) and the chronic period (after the latent period) (24). Only those spontaneous behavioral seizures exhibited after the latent period were defined as TLE-SRS.

The study was divided into 3 parts. The first part consisted of identifying the internal control of PSD protein among β-actin, β-tubulin, and GAPDH and to assess the dynamic change of α-tubulin and β-tubulin in the epileptic hippocampus at different stages of the model. In this part, animals were randomly assigned into the experimental seizure group or the control group. Control animals received a similar volume of 0.9% saline rather than pilocarpine hydrochloride, with other conditions and treatments being the same as those of the seizure group. All animals were monitored utilizing video-scalpel electroencephalogram (EEGs) from 2 days before both interventions, as previously described (35,37), with the exception that our videos were taken from 8 a.m. to 8 p.m, and EEGs were conducted for 24 h. Rats were randomly sacrificed respectively at 1, 3, 7, 15, and 30 days (defined as the D1, D3, D7, D15, and D30 groups, respectively) after pilocarpine injection for the seizure group or at 1 day after saline injection for the control group.

The second part of the study required distinguishing the expression differences of PSD MTs between animals who suffered from chronic SRS and those who did not. The method of video-scalpel EEG monitoring and the preparation of the control group was conducted as the first part. Animals were all sacrificed on the 60th day, and hippocampus slices were examined using Western blot (WB), Nissl staining, or immunoelectron microscopy to see if there were differences in cell loss of the hippocampus and α- and β-tubulin expression among TLE-SRS, TLE-NSRS,

and control group.

For the third part, 72 animals were first randomly assigned into groups with different dosages of colchicine (coc) or paclitaxel (pac), stereotactically injected into the hippocampus. The optimal doses of the 2 drugs were established based on hippocampal neuron status according to Nissl staining and β-tubulin expression 7 days later. After that, the chosen dose of colchicine, paclitaxel, or the same amount of saline was randomly injected into the hippocampus of 60 rats on the 7th day after pilocarpine-induced SE (50 min or longer). Then, animal behaviors and scalp EEGs were monitored for the next 30 days. Based on whether SRS developed, the rats were classified into coc-TLE-SRS, coc-TLE-NSRS, pac-TLE-SRS, pac-TLE-NSRS, TLE-SRS, and TLE-NSRS groups.

Since the minimum number of each subgroup was 3, in all 3 parts, if the sample size of subgroups was insufficient due to the model's failure or death of animals, a complement of rats was added randomly.

PSD purification

Rats were deeply anesthetized with 10% chloral hydrate (3 mL/kg, i.p.), and then the whole brains were extracted, weighed, and quickly placed in liquid nitrogen. Ten grams of whole-brain tissue was transferred to a grinding bowl pre-cooled by liquid nitrogen, merged into ice-cold lysis buffer A (0.32 M sucrose, 1 mM NaHCO3, 1 mM $MgCl_2$, 0.5 mM $CaCl_2$, Co. ShanPu, Shanghai, China) (2 mL per gram of brain) and 1× protease inhibitors (Co. KangCheng, Shanghai, China), and then ground into homogenate. To obtain pure PSD protein, a subsequent procedure which has been previously described (38,39), was conducted. During this process, part of the supernatant pellet P2 (crude membrane fraction) and synaptosome (SynT) was kept for checking the purity of PSD.

Western blot analysis

WB was performed as previously described (40,41), with a slight change in the utilization of the BCA Protein Assay Kit (KPL, USA). Proteins were run on polyacrylamide gels at 100 to 150 V for 2 h and were then electrotransferred to polyvinylidene difluoride filter (PVDF) membrane at 80 V for 120–180 min or at 60 mA overnight. The membrane was blocked for 2 h at room temperature within 0.1% phosphate-buffered saline (PBS) with 3% bovine serum albumin (BSA) and 5% non-fat milk. After that, the PVDF was incubated overnight at 4 ℃ with primary antibodies against synaptophysin, NMDA receptor subunit 1 (Chemicon, Rolling Meadows, IL, USA) or antibodies against PSD-95, β-actin, GAPDH, α-tubulin, and β-tubulin (Santa Cruz, CA, USA) (diluted from 1:200 to 1:2,000, respectively). After washing 4 times with buffers, the PVDF was incubated with secondary goat anti-rabbit IgG (Santa Cruz) (1:2,000) for 60 min at room temperature. Finally, immunolabelled bands were quantified from scanned images using the image analysis software Image-Pro Plus 6.0, as described previously (37).

Immunoelectron microscopy

Animal anesthetization, fixation, and tissue preparing for immunoelectron microscopy were performed as described previously (22,42). Briefly, the hippocampal dentate gyrus (DG) was dissected under a microscope according to the rat brain's anatomy (43). After fixing in 2.5% glutaraldehyde, the brain was washed a few times in PBS, postfixed in 2% osmium acid solution for 2 h, and dehydrated for 5 min each time using 50%, 70%, 90%, and 100% acetone solution in order. Then, it was soaked in an equal volume of epoxy resin and pure acetone mixture, and embedded in the agent of 51 mL Epon812, 12 mL DDSA, 37 mL MNA, and 2 mL DMP-30 (Sigma-Aldrich) at 60 ℃ for overnight. After that, the tissue was cut to slices with a thickness of about 50–70 nm using a cryogenic microtome (American Optical, USA). Slices were collected on mesh nickel grids, soaked in 1% H_2O_2 for 10 min to 1 h (depending on the hardness of the resin and the thickness of the chip) in order to wash out osmium acid and to enhance the resin's penetration for antibodies. After 3 times washing in double distilled water, slices were pre-incubated in 1% normal donkey serum for 30–60 min at room temperature, followed by another 3 min of PBS wash. Sections were then incubated with the primary anti-β-tubulin (1:50, Santa Cruz, CA, USA) for 1 h at room temperature and 24–36 h at 4 ℃. After rinsing in PBS, sections were incubated in PBS with 1% BSA (PH8.2) for 5 min and then in gold-labeled goat anti-rabbit antibody (1:100, Sigma-Aldrich) for 10 min to 1 h at room temperature. Slices were then washed and disposed of in uranium acetate and uranium citrate respectively for 5 min, with more washes in between and after. A Hitachi H-600 transmission electron microscope (TEM) was used to observe the synaptic and expression of PSD particles in

the hippocampal CA1 area under 50,000× magnification. Twenty pictures were taken from each animal. Labeling and minor adjustments in contrast and brightness were made using Adobe Photoshop (CS, Adobe Systems, San Jose, CA, USA).

Nissl staining

The coronal brain hippocampus was cut to 20 μm slices using a cryogenic microtome (American Optical, USA). Anatomical landmarks were used according to the brain atlas to ensure hippocampal sections were matched between groups. Every third slice was selected, and 4 slices were taken from each animal. The selected brain sections were rinsed with distilled water and stained with 0.1% tar violet at room temperature for 10 min. If overstaining occurred, 95% ethanol would be added for discoloration. Slices were then washed and dehydrated using 70% ethanol for 3 min, 95% ethanol for 3 min, along with 3 washes of 100% ethanol (1 min each time) and 2 washes of xylene twice (5 min each time), and then sealed with neutral resin. Images of the sections were captured using a Leica light microscope (Leica dM5000 B), and the mean normal vertebral cell numbers in the area of CA1, CA3 and DG were calculated and analyzed using the ImagePro Plus 6.0 software package (IPP 6.0, Media Cybernetics, USA) by 2 investigators in a blinded manner.

Brain surgery and hippocampus injection

Animals were deeply anesthetized with 10% chloral hydrate (3 mL/kg, i.p.) and fixed on a stereotaxic apparatus (RWD Life Science, Shenzhen, China). Responsiveness to pain was checked every 15 min by toe pinch. The head skin and scalp dissection was conducted as previously described (35). Next, 1 μL colchicine (with different dosages of 0.01, 0.03, 0.1, 0.3, 1.0, and 2.0 mg), 1 μL paclitaxel (with different dosages of 0.1, 0.5, 1.0, 1.5 mg), or 1 μL saline was stereotactically injected into each side of the hippocampus using the following coordinates (all in mm relative to bregma): anteroposterior (AP) −3.3, mediolateral (ML) ±1.8, superior-inferior (SI) −3.3, and AP −4.7, ML ±5.3, SI −5.5. Flow speed was controlled at 0.1 μL/mL by stereotactic microinjector (KDS, Legato 130, USA), with the syringe tip remaining in the site for 5 min after injection to ensure solutions were thoroughly absorbed. Animals were then sutured and kept warm using a heating pad before recovering from anesthesia. All rats survived and remained active post-surgery.

Statistical analysis

Experimental data were presented as the mean ± standard deviation (SD). The comparison of average data between multiple groups was conducted by applying a one-way analysis of variance (ANOVA) followed by Scheffe's post hoc test. Differences between the experimental group and control group at different stages were calculated using an independent samples *t*-test after a normality test and homogeneity of variance test. SPSS version 18.0 (SPSS Inc., Chicago, IL, USA) was applied for statistical analyses, and Microsoft Office Excel 2003 (Microsoft, USA) was used for plotting diagrams. P value <0.05 was considered statistically significant.

Results

Animal modeling

In the first part of the study, 23 rats were randomly chosen from a group of 203 rats for saline injection as controls, and did not display any epileptiform convulsions in behavior. Among the remaining 180 pilocarpine injected rats, almost 80% of the rats developed a SE after two injections of pilocarpine, and the average dose of pilocarpine-induced SE was 27.14 mg/kg (range, 20–50 mg/kg). Overall, 164 rats (91.1%) exhibited racine III–V seizures and developed to SE, in which 21 rats died because of SE, and another 16 died after seizures due to other reasons (the mortality rate was 20.6%). The surviving rats began to exhibit spontaneous partial to tonic-clonic seizures, which lasted from about 30 s to 1 min beginning the 15th day, and the number of seizures varied from one to several times a day. No rats died in this chronic period.

In the second part of the study, 200 rats were used for the seizure group, and 36 rats were used for control. Among these 200 pilocarpine-injected rats, 182 (91%) showed Racine III–V seizures and developed to SE, of which 145 rats survived to 60 days (the mortality rate was 27.5%). There were altogether 101 rats that exhibited spontaneous seizures mostly beginning the 15th day, which manifested from a short duration of nodding, bristling, clonus of forelimb, and falling (Racine I–III) to longer secondary generalized or tonic-clonic seizures (Racine IV–V), with seizure numbers also varying from one to several times a day. We defined animals with these behaviours as the TLE-SRS group. Another 44 rats (22%) that did not exhibit seizure activities throughout the observation, were defined as the TLE-NSRS group. Controls did not exhibit any

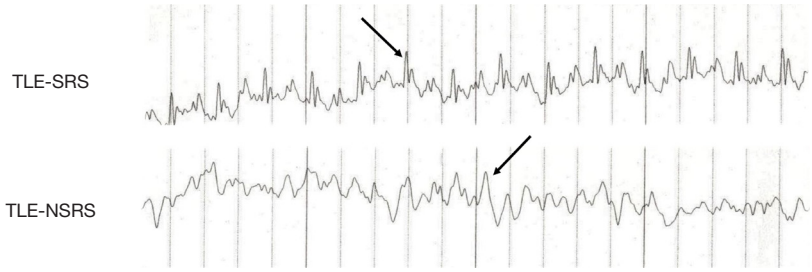

Figure 1 EEG monitoring trace examples of TLE-SRS and TLE-NSRS group. The black arrows indicate the difference between the two typical sharp waves of the two groups. EEG, electroencephalogram; TLE, temporal lobe epilepsy; SRS, spontaneous recurrent seizure.

epileptiform convulsion behavior in this part.

Based on these mortality rates and the minimum animal number's rule, rats were supplemented for the later experiments if animals died, and the final animal numbers recruited in each group are reported in each figure.

EEG recordings

Different phases of the inter-ictal period had different EEG characteristics. Generally, there was single or multiple, or burst of spikes together with increased theta rhythm observed during the first 24 h after pilocarpine injection (acute phase). EEGs between the 3rd and 14th day (latent phase) were generally healthy. Sporadic sharp waves, spike waves, or slow spike complex waves were noticed much more frequently from the 15th to 60th day (chronic phase). There was no spontaneous seizure nor any EEG-recorded epileptiform discharges in the saline control group. For later experiments, TLE-SRS animals all exhibited increased theta rhythm and more single, multiple, or burst of spikes, but the TLE-NSRS animals displayed normal or mild abnormality on EEG, with scattered spikes or sharp waves (*Figure 1*).

GAPDH was more reliable as an internal control for western blot analysis of PSD protein in pilocarpine TLE rat models

To find a good internal control for PSD protein, β-actin, β-tubulin, and GAPDH were tested in different time points in the experimental group and the control group using WB. Since synaptophysin (SynPhy) was a presynaptic component, and NMDA receptor 1 (NR1) and PSD-95 were postsynaptic components, they were respectively checked in PSD, supernatant pellet P2, and synaptosome (SynT) to assess the purity of PSD. It was found that NR1 and PSD-95 were all expressed in PSD, SynT, and P2, while SynPhy was only expressed in SynT and P2 but not PSD (*Figure 2A*), confirming a high purity of the extracted PSD. WB showed that β-actin, β-tubulin and GAPDH were detected in all groups. Compared to control, the relative expression of β-actin and β-tubulin (I) was decreased in the D1 group (92%±11%/96%±7%) but without statistical significance (both P>0.05); and (II) decreased in the D3 group (72%±8%/ 68%±12%) (both P<0.05), with the lowest level in the D7 group (14%±1%/24%±3%) (both P<0.01), and slowly increasing in the D15 group (27%±10%/44%±11%) and D30 group (41%±9%/50%±10%) (P all <0.01). In contrast, GAPDH was relatively stable following SE, with the expression level of 106%±17%, 111%±17%, 97%±15%, 101%±21%, and 93%±12% relative to the control group in the D1–D30 groups, respectively (P all >0.05; *Figure 2B*,*C*). To avoid errors of sample application, 2 samples were randomly taken out from each of the D15 and control group and loaded 6 times into adjacent channels for examinations of β-actin, β-tubulin, and GAPDH. WB showed that there was still a significant decrease of β-actin and β-tubulin in the D15 group (0.27±0.12/0.46±0.11) compared with the control group (both P<0.05), while the expression of GAPDH was again stable (0.97±0.11, P>0.05) (*Figure 2D*,*E*), indicating that the error of sample application was overcome and GAPDH could be the internal control for PSD protein.

α- and β-tubulin of PSD both decreased from the third day after pilocarpine-induced seizures

WB showed that α- and β-tubulin of PSD were both decreased significantly in the D3 (0.41±0.06/1.14±0.09, both P<0.05), D7 (0.14±0.01/0.62±0.03, both P<0.01), D15 (0.23±0.10/0.86±0.11, both P<0.01) and D30 group

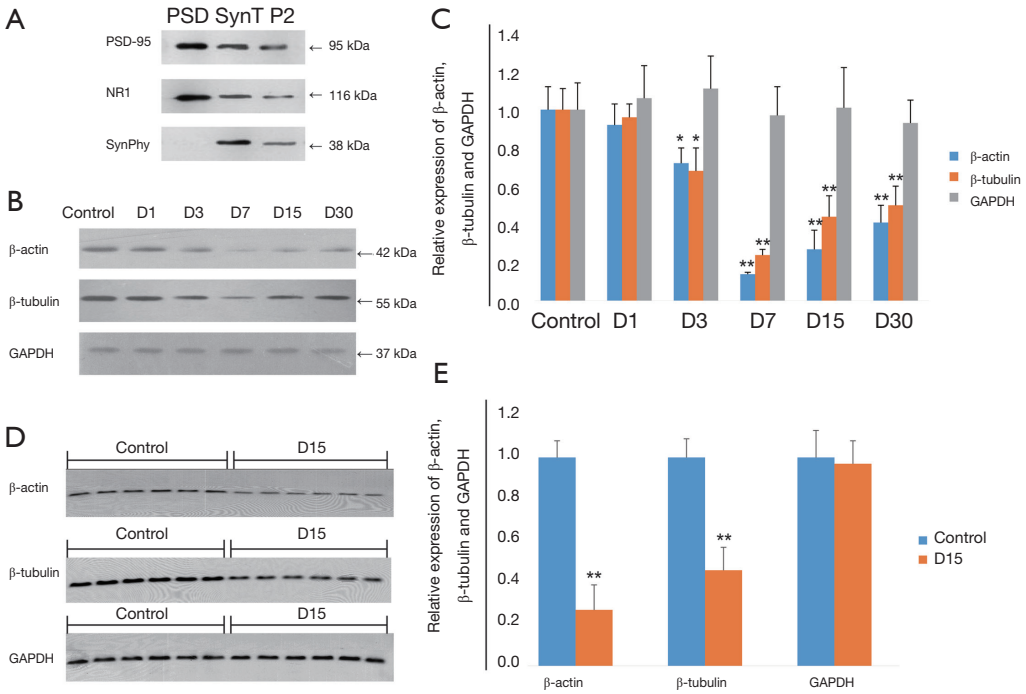

Figure 2 The purity test and the internal control orientation of PSD protein. The purity of PSD was evaluated by Western blot as shown in (A). The expression of β-actin, β-tubulin and GAPDH at different time points of the pilocarpine-injected experimental groups and the control group was tested by Western blot as shown in (B), and the data analysis is shown in (C,D). One sample randomly took from the control group. Another sample randomly took from the D15 seizure group was tested for β-actin, β-tubulin, and GAPDH; each sample was then loaded into 6 channels to exclude the loading error. Data analysis is shown in (E). The animal number for (A), (B), and (C) was 20 for each group. Error bars are SEM. *, P<0.05; **, P<0.01. PSD, postsynaptic density.

(0.38±0.09, P<0.01; 1.16±0.10, P<0.05) compared with the control group (0.78±0.11/1.61±0.21). There was difference in the expression of α-tubulin and β-tubulin between the D1 group and the control group (0.72±0.08/1.49±0.11, P>0.05) (*Figure 3A,B*). Immunoelectron microscopic examination also found that compared to the control group, β-tubulin particles in PSD had noticeably reduced to 71%±9% (P<0.05), 3%±2% (P<0.01), 26%±11% (P<0.01) and 38%±10% (P<0.01) respectively in the D3, D7, D15, and D30 groups, as confirmed in WB tests. There was also difference in the expression of β-tubulin in the D1 group (0.98±0.11) or the control group, with its lowest level also being present in the D7 group (almost no β-tubulin granules in PSD) (*Figure 3C,D*).

The TLE-NSRS group and the TLE-SRS groups in particular experienced gippocampal neuron loss

Nissl staining showed that dense pyramidal cells and granular cells were neatly arranged in CA1, CA3, and the DG in control animals. The neurons in the boundary of hilus were large, with clear outlines and abundant cytoplasm Nissl bodies. However, neurons of the CA1 and CA3 from the TLE-SRS group showed a disorderly arrangement and incomplete morphology, with swollen or shrunken cell bodies, unclear boundaries, enlarged intercellular space, and decreased amounts of cytoplasmic Nissl bodies. There were also irregular boundaries and different arrangements of granular cells in DG. Statistical analysis showed that the neuron numbers in the hippocampal CA1 (109±10), CA3 (112±7), and DG (126±7) of the TLE-SRS group were much lower than those of the control group (256±11, 278±10, and 268 ±10, respectively, P all <0.01). Also, the neuron measures in the 3 regions of the TLE-NSRS group (186±15, 192±6, 203±6, respectively) were significantly more reduced than those of the control group (P all <0.01), but these were still more numerous than those in the TLE-SRS group (P all <0.01) (*Figure 4*).

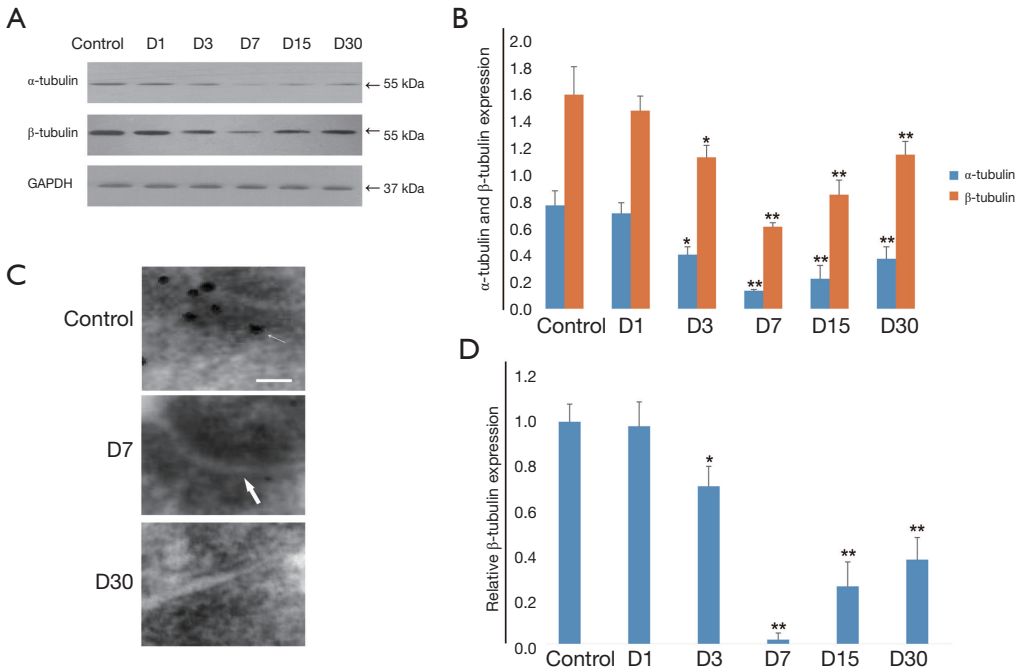

Figure 3 Expression comparison of α-tubulin and β-tubulin between the seizure groups and control group. (A) The expression of α-tubulin, β-tubulin, and GAPDH at the different time points of pilocarpine-injected experimental groups and the control group was tested by Western blot, with the data analysis result shown in (B,C). The expression of β-tubulin was also examined using the immunoelectron microscopic method, with the data analysis result shown in (D). A thicker white arrow represents PSD structure, and a thinner arrow represents β-tubulin particles. Scale bar: 100 nm. The animal number for (A,B) and (C,D) was 3 for each group. Error bars are SEM. *, P<0.05; **, P<0.01.

α- and β-tubulin expression were both downregulated in TLE-SRS and TLE-NSRS groups

WB showed that the expression of PSD α- and β-tubulin in the TLE-SRS group (0.23±0.08/0.53±0.09) was significantly lower than that of the control group (1.19±0.21/1.89±0.16; both P<0.01) and that of the TLE-NSRS group (0.66±0.13/1.07±0.12; both P<0.01). There were also significant differences between the TLE-NSRS group and the control group (P<0.05) (*Figure 5A,B*). To confirm this result, immunoelectron microscopic examination of β-tubulin in PSD of the three groups was conducted. It was determined that the β-tubulin in the TLE-SRS group and TLE-NSRS group declined to 17%±3% and 52%±12% compared to the control group (P<0.01). There was also statistical difference between the TLE-SRS group and the TLE-NSRS group (P<0.01) (*Figure 5C,D*).

Orientation of the optimized dose of colchicine for intervention

Animals were sacrificed 7 days after the injection of different doses of colchicine or saline, and Nissl staining and WB was applied to see which dose of colchicine caused more depolymerizations of microtubules and less neuron loss. Representative examples of Nissl staining and WB images are shown in *Figure 6A*. It turned out that compared with the control group, no significant difference in DG cell counts was observed in the coc-0.01 μg (105%±15%), coc-0.03 μg (103%±11%), coc-0.1 μg (105%±10%) and coc-0.3 μg (98%±9%) groups (all P>0.05), but there was significant difference in the coc-1.0 μg (43%±18%) and coc-2.0 μg (24%±11%) groups (both P<0.01) (*Figure 6B*). No significant difference in PSD β-tubulin expression was detected in the coc-0.01 μg (91%±21%), coc-0.03 μg (102%±17%), or coc-0.1 μg (95%±8%) group

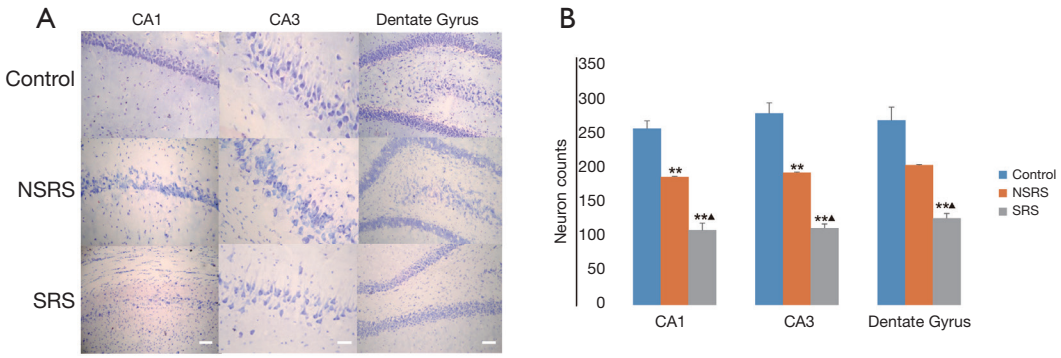

Figure 4 Nissl's staining of neuron loss in the hippocampus. Scale bars represent 50, 20, and 100 μm respectively in (A). n=3 for each group of (B). **, compared to the control group, P<0.01; ▲, compared to the TLE-NSRS group, P<0.01.

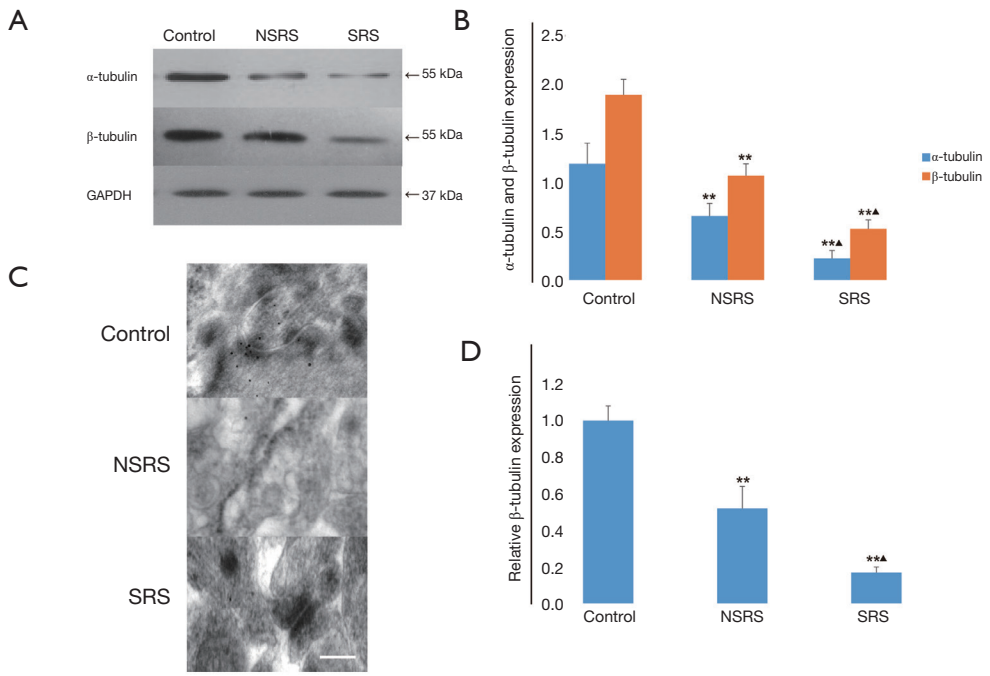

Figure 5 Expression comparison of α-tubulin and β-tubulin among TLE-SRS, TLE-NSRS, and control groups. N=20 for each group of (A) and (B); n=3 for each group of C and D. Scale bar represents 500 nm in (C). **, compared to the control group, P<0.01; ▲, compared to the TLE-NSRS group, P<0.01. TLE, temporal lobe epilepsy; SRS, spontaneous recurrent seizure.

(all P>0.05), but there was significant difference in the coc-0.3 μg (61%±11%), coc-1.0 μg (45%±8%), and coc-2.0 μg (36%±11%) groups (all P<0.01) (*Figure 6C*). Based on these data, coc-0.3 μg was considered the optimized dose of colchicine, which could cause depolymerization of microtubules without neuron loss.

Orientation of the optimized dose of paclitaxel for intervention

Representative examples of Nissl staining and WB images are shown in *Figure 7A*. In this study, no significant difference in DG cell counts was found between the pac-

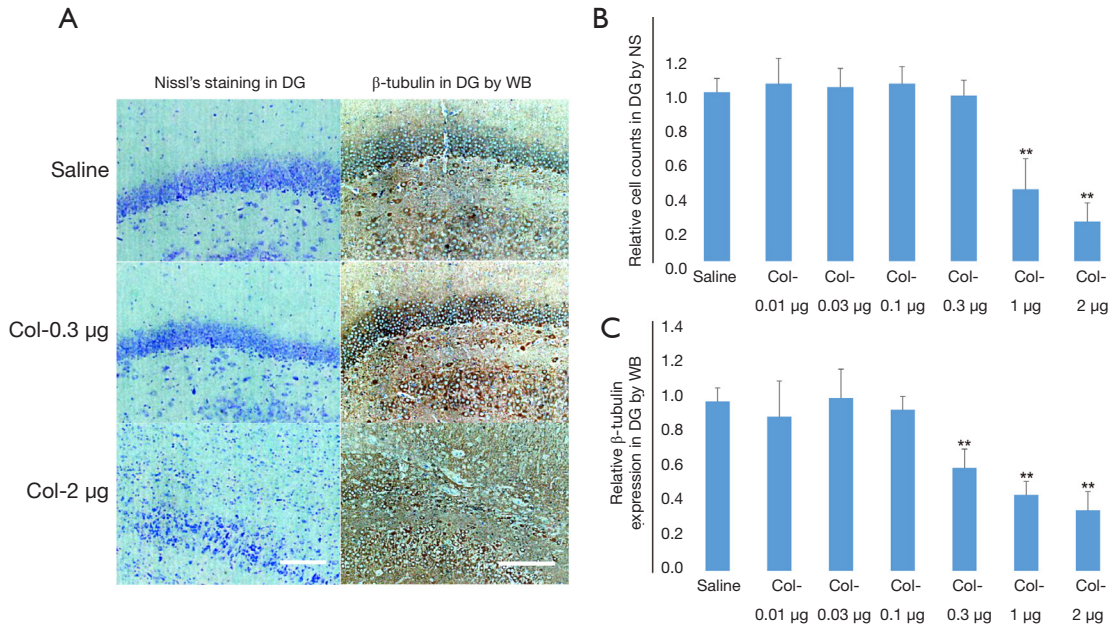

Figure 6 The orientation of the optimized dose of colchicine injected into the hippocampus. Scale bar represents 100 μm in (A). n=3 for each group of (B) and (C). **, P<0.01.

0.1 μg (102%±13%), pac-0.5 μg (98%±8%), and pac-1.0 μg (103%±21%) groups versus the saline control group (P all >0.05), but the pac-1.5 μg group, which decreased to 34%±17%, did significantly differ from the saline control group (P<0.01) (*Figure 7B*). For the WB examination, no statistical difference in β-tubulin expression was detected between pac-0.1 μg (103%±12%) and pac-0.5 μg group (97%±9%), and the control group (both P>0.05). However, compared with the control group, the β-tubulin expression in the pac-1.0 μg group increased to 138%±11%, while that of the pac-1.5 μg group decreased to 35%±18% (both P<0.01) (*Figure 7C*). Therefore, pac-1.0 μg was considered the optimized dose of paclitaxel because it caused the increase of PSD β-tubulin (polymerizations of microtubules) without neuron loss.

There were no epileptic seizures or behavioral changes seen in the colchicine or paclitaxel intervention groups, and their EEGs were normal, suggesting that the two drugs themselves were not epileptogenic.

Paclitaxel diminished the chronic SRS rate and increased the expression of PSD β-tubulin in the rat pilocarpine TLE model

On the seventh day after pilocarpine-induced SE, 60 rats were randomly assigned to groups respectively receiving 1 μL of saline, 0.3 μg colchicine, or 1.0 μg paclitaxel injected into two sides of the hippocampus. After 30 days, 15 in 20 saline-injected TLE rats, 18 in 20 coc-0.3 μg-injected rats, and only 8 in 20 pac-1.0 μg-injected rats exhibited SRS. Data analysis showed there were statistical differences between the pac-1.0 μg group and the other two groups (both P<0.01; *Figure 8A*). Immunoelectron microscopy analysis also found that more β-tubulin particles were found in the pac-1.0 μg-TLE-SRS group (3.5±0.21) than the saline-TLE-SRS group (1.10±0.11) and the coc-0.3 μg -TLE-SRS group (0.71±0.08) (both P<0.01; *Figure 8B,C*). There were no statistical differences of β-tubulin expression among groups of saline-TLE-NSRS, coc-0.3 μg-TLE-NSRS, and pac-1.0 μg-TLE-NSRS (P all >0.05) (*Figure 8B,C*). Moreover, there were lower amplitude and less single, multiple or bursts of continuous spike waves seen in the pac-1.0 μg-TLE-SRS group than in the saline-TLE-SRS group and coc-0.3 μg-TLE-SRS group (*Figure 9*), and there was not much difference in EEG abnormal spike waves detected among the saline-TLE-NSRS, coc-0.3 μg-TLE-NSRS and pac-1.0 μg-TLE-NSRS group (data not shown).

Discussion

SRSs, which occur in pilocarpine-treated rats after the latent period and appear to recur in a clustered way (44,45),

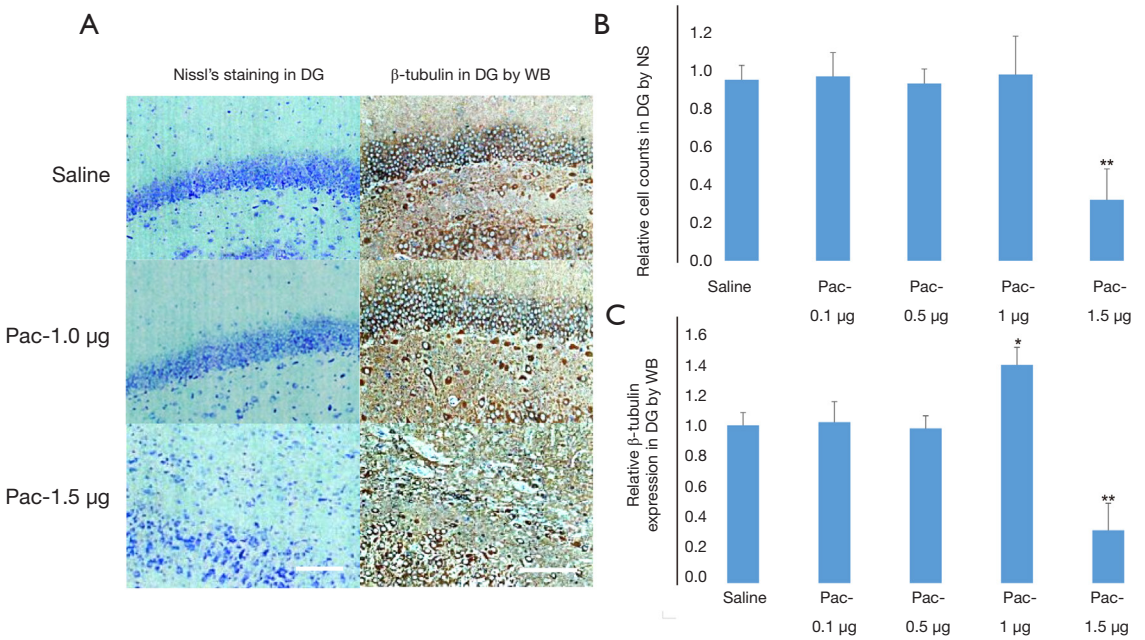

Figure 7 The orientation of the optimized dose of paclitaxel injected into the hippocampus. Scale bar represents 100 μm in (A). n=3 for each group of (B) and (C). *, P<0.05; **, P<0.01.

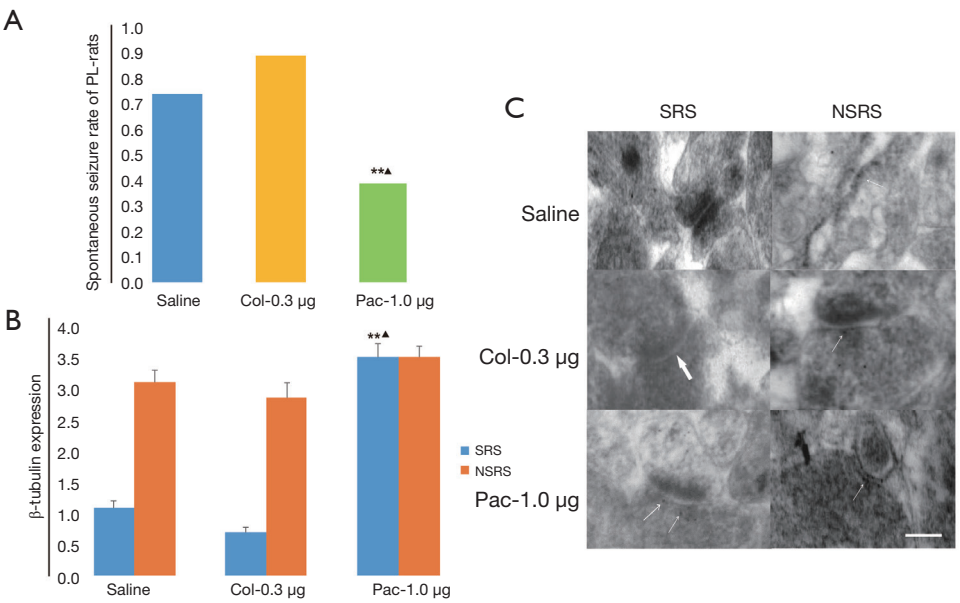

Figure 8 The change of SRS rate and β-tubulin expression after intervention by coc-0.3 μg and pac-1.0 μg. (A) n=20 for each group; there were 15 saline-injected TLE rats, 18 coc-0.3 μg-injected rats, and only 8 pac-1.0 μg-injected rats that exhibited SRS. The immunoelectron microscopy data analysis is shown in (B), with immunofluorescence staining image examples shown in (C). The thicker arrow represents the location of PSD. Thiner arrows represent β-tubulin particles. **, compared to the saline control group, P<0.01; ▲, compared to the coc-0.3 μg-TLE-SRS group, P<0.01. n=3 for each group. Scale bar represents 500 nm. TLE, temporal lobe epilepsy; SRS, spontaneous recurrent seizure.

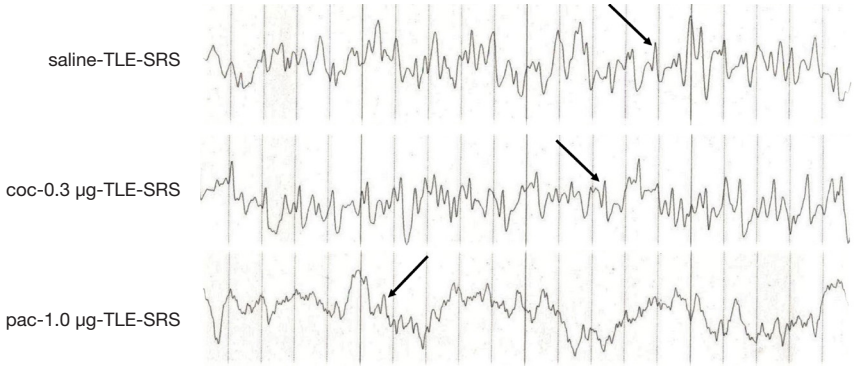

Figure 9 EEG monitoring trace examples of TLE-SRS animals pretreated with saline, coc-0.3 μg and pac-1.0 μg. As typical sharp waves show in different groups (black arrows), the pac-1.0 μg-TLE-SRS animal showed less frequent and lower amplitude sharp waves than the other two groups. EEG, electroencephalogram; TLE, temporal lobe epilepsy; SRS, spontaneous recurrent seizure.

are highly isomorphic in human disease, and as such, are a suitable tool for investigating the pathophysiogenetic mechanisms of TLE. The initial reaction of the model like febrile convulsion or status epilepticus can prompt a complex and orderly response of neuron death, glial cell proliferation, mossy fiber sprouting, rewiring of synaptic circuits, neurogenesis, and axonal dendritic and synaptic remodeling, to reconstruct the impaired neural networks and fix nervous system damage (46,47). Even though these changes also exist during the latent and chronic periods, there is no definitive evidence that any of these phenomena are critical for epileptogenesis (48,49). Furthermore, not every latent animal would develop to SRS. It is believed that during the latent period, several epileptogenesis-related pathophysiological phenomena may be present, and when the threshold is exceeded, SRSs occur. Thus, it is necessary to further investigate the underlying mechanism in the latent period extension.

Microtubules have been reported to be important in the maintenance of cell morphology, the generation and orientation of neurite outgrowth, the differentiation and migration of cells, neuronal polarity, tissue distribution and apoptosis (50). Studies have confirmed that α- and β-tubulin are widely present in PSD (51), and the destruction of microtubules can directly affect the morphology and protein composition of PSD, which also could alter the synaptic effect (52). In the present study, we found that the expression of PSD α- and β-tubulin were both downregulated significantly in the latent and chronic period, especially on the seventh day, which is consistent with previous studies in line with the timeline of reported extensive hippocampal neuron loss after SE (16,20,53,54). We could deduce from this that there is PSD structure damage after SE and self-reconstruction after the most severe injury. Moreover, we found a significant decrease in PSD microtubules and hippocampal neuron numbers in both the TLE-SRS and the TLE-NSRS group compared with the control group (especially in the TLE-SRS group), suggesting that the downregulation and the depolymerization of microtubules may be one of the mechanisms of programmed death of hippocampal neurons induced by SE and SRS. There may be a negative correlation between the expression of microtubules and the SRS rate: the more microtubules are depolymerized, the more likely it is that animals develop SRS.

The decrease of microtubules and their roles in neuron death has still not been thoroughly investigated. It is hypothesized that the phosphorylation and oxidation of microtubules could cause their depolymerization, destroy the cytoskeletal structure, and disintegrate neurons. Also, the decrease of microtubules could down-regulate the expression of Bcl-2, which may ultimately lead to apoptosis through the activation of Bax/Bak, the release of mitochondrial cytochrome C, and then the activation of caspases (50,55).

Many studies have attempted to ascertain whether repeated spontaneous seizure is a mechanism behind neuronal death after SE, or whether the severity of neuronal cell death after SE determines if there is a subsequent spontaneous seizure. For example, Gorter *et al.* used a TLE rat model to discover that the degeneration and necrosis of most neurons occur in the first week after SE, and the degree of cell death is closely related to SE's duration. There was no significant difference in TUNEL positive

cells between the progressive SE group (with spontaneous seizures more than 8 times a day) and the non-progressive SE group (1–2 seizures a week on average), suggesting that hippocampal neuron death was not correlated to the frequency of chronic SRS but was the consequence of initial seizure (56). Deshpande *et al.* further investigated the direct influence of persistent and intermittent epileptic discharge on neuronal death *in vitro* and confirmed that the continuous high-frequency epileptic discharges were associated with cell death in a time-dependent manner, but were not sufficient for subsequent recurrent spontaneous epileptiform discharges (48). Moreover, the timeline of microtubule recovery was also consistent with that of the mossy fiber sprouting after SE (57,58), revealing that microtubules may be involved in synaptic remodeling by participating in mossy fiber sprouting. We therefore speculated that though hippocampal neuron death after SE is not directly relevant to chronic SRS, its severity still may indirectly determine whether SRS occurs through affecting synaptic remodeling.

As of now, the mechanism of decreased microtubules induced by SE remains unclear. Some have postulated that it may be due to the massive influx of Ca^{2+} after SE (59). *In vitro* studies have confirmed that the increase of intracellular Ca^{2+} level can cause microtubule depolymerization through postsynaptic Ca^{2+}-CaM signaling pathways (60), thus affecting cell movement, axon transportation, and even cell survival. Another reasonable interpretation may be referred to as "tubulin code", which theorizes that SE could cause a decrease in microtubules by changing the composition of their isotypes or through post-translational modification (13). It was also reported that the activation of CaMK II in PSD can induce phosphorylation of microtubules *in vitro* (61).

Furthermore, the overexpression of nitric oxide (NO), peroxynitrite ($ONOO^-$), and superoxide anions under oxidative stress can induce the oxidation and nitration of microtubules. These stresses also could promote microtubule's decomposition and depolymerization (62). Since seizures can activate iNOS and produce oxidative stress response (63), we speculate that the phosphorylation, oxidation, and nitration of microtubules together with CaMK II signaling pathway all participate in the depolymerization of microtubules, which leads to the damage of PSD skeletal structure and the efficiency of synaptic function.

There are also interactions between NMDA receptors (NRs) and microtubules (64). It has been reported that NRs need to be transported to the postsynaptic membrane with the help of microtubule before combining with glutamate to work. Additionally, a downregulation of PSD NR1 and NR2A/B receptors in tissue specimens from patients with refractory epilepsy (65), along with a kainite-induced mesiotemporal lobe epilepsy model (38,66), was detected when compared with their respective controls. Combining the findings with our own research, we speculate that microtubules may play a role in interfering with the plasticity of epileptogenic synapses after SE through the dysregulation of NR expression and function.

Paclitaxel has already been confirmed to be effective in Alzheimer's disease (AD) and autoimmune encephalomyelitis (EAE) due to its role in stabilizing microtubules (67-69). Our study showed that low-dose paclitaxel lowered the chronic SRS rate and increased the expression of PSD β-tubulin in this TLE model, strongly suggesting to us that paclitaxel may be a neuroprotective agent against SRS. However, the specific mechanism underlying this is still not clear. It was reported that normal microtubules play a role in limiting Ca^{2+} influx. Slightly elevated intracellular calcium level was found to be fundamental to the regulation of microtubule depolymerization, cell motility, and axonal transportation, but excessive Ca^{2+} influx under excitotoxic conditions was shown to be fairly harmful or even lethal to neurons. We speculate that the large amount of Ca^{2+} influx induced by SE could lead to the decomposition and depolymerization of microtubules, and the collapse of the microtubule system could further promote the influx of Ca^{2+}, increase the excitability of neurons, and ultimately aggravate the development of epilepsy. *Ex vivo* study has confirmed that paclitaxel can limit Ca^{2+} influx and inhibit the decomposition of microtubules incurred by AMPA, NMDA, or KA receptors, thereby alleviating glutamate neurotoxicity and protecting neurons from death (70). It was also reported that the molecular motor KIF5A, one of the microtubule-dependent molecular motors critical for neuronal function, is essential for $GABA_A$ receptor transportation, and the deletion of KIF5A could lead to epilepsy. Since we know GABA transmission plays an important role in the genesis and propagation of epileptic activity, we can surmise that GABA transmission may also be another reasonable pathway. These findings link microtubules to the mechanism of neurotoxicity and GABA/glutamate transmission, and likewise warrant further investigation.

There limitations to this study should be addressed. For example, we failed to test the expression of α-tubulin by

immunoelectron microscopy. Also, there were a limited number of samples in the specific sub-groups, while the intervention reagents we used in this work (colchicine and paclitaxel) were themselves of central toxicity. Future experiments should focus on minimizing these limitations, optimizing the intervention drugs, and looking deeper into the function and mechanism involved. It would be of great value to further confirm the changes observed in animals via biopsy specimens from pharmacoresistant TLE patients who have undergone epilepsy surgery.

In conclusion, this study suggested that microtubules may be involved in the development of hippocampal neuronal apoptosis and SRS of this lithium-pilocarpine TLE rat model in an extent-dependent manner. Though the mechanisms are not well understood, targeting the neuronal microtubules still may provide new insights into the pathogenesis of epilepsy and could be taken as a potential treatment and prevention strategy for this illness.

Acknowledgments

Funding: This work was supported by the National Natural Science Foundation of China (81601140, 81601141).

Footnote

Reporting Checklist: The authors have completed the ARRIVE reporting checklist. Available at http://dx.doi.org/10.21037/atm-19-4636

Data Sharing Statement: Available at http://dx.doi.org/10.21037/atm-19-4636

Peer Review File: Available at http://dx.doi.org/10.21037/atm-19-4636

Conflicts of Interest: All authors have completed the ICMJE uniform disclosure form (available at http://dx.doi.org/10.21037/atm-19-4636). The authors have no conflicts of interest to declare.

Ethical Statement: The authors are accountable for all aspects of the work in ensuring that questions related to the accuracy or integrity of any part of the work are appropriately investigated and resolved. All procedures of this investigations were conducted under approved protocols of Central South University (Changsha, China) Institutional Review Board and were performed in compliance with the National Institutes of Health Guide for the Care and Use of Laboratory Animals (NIH publications, Version 1996) and the ARRIVE Guidelines. The study was reviewed and approved by the Animal Ethical and Welfare Committee and the Institutional Animal Care and Use Committee (IACUC), The Second Xiangya Hospital, Central South University, China (Approval No. 2020093).

References

1. Moshé SL, Perucca E, Ryvlin P, et al. Epilepsy: new advances. Lancet 2015;385:884-98.
2. Manford M. Recent advances in epilepsy. J Neurol 2017;264:1811-24.
3. Long LL, Song YM, Xu L, et al. Aberrant neuronal synaptic connectivity in CA1 area of the hippocampus from pilocarpine-induced epileptic rats observed by fluorogold. Int J Clin Exp Med 2014;7:2687-95.
4. Kaila K, Ruusuvuori E, Seja P, et al. GABA actions and ionic plasticity in epilepsy. Curr Opin Neurobiol 2014;26:34-41.
5. Cavazos JE, Cross DJ. The role of synaptic reorganization in mesial temporal lobe epilepsy. Epilepsy Behav 2006;8:483-93.
6. Barnes GN, Slevin JT. Ionotropic glutamate receptor biology: effect on synaptic connectivity and function in neurological disease. Curr Med Chem 2003;10:2059-72.
7. Frank RA, Grant SG. Supramolecular organization of NMDA receptors and the postsynaptic density. Curr Opin Neurobiol 2017;45:139-47.
8. Sheng M, Kim E. The postsynaptic organization of synapses. Cold Spring Harb Perspect Biol 2011;3:20.
9. Terenzio M, Schiavo G, Fainzilber M. Compartmentalized Signaling in Neurons: From Cell Biology to Neuroscience. Neuron 2017;96:667-79.
10. Hegde AN, DiAntonio A. Ubiquitin and the synapse. Nat Rev Neurosci 2002;3:854-61.
11. Leitner MG, Halaszovich CR, Ivanova O, et al.

Phosphoinositide dynamics in the postsynaptic membrane compartment: Mechanisms and experimental approach. Eur J Cell Biol 2015;94:401-14.
12. Haas KF, Miller SL, Friedman DB, et al. The ubiquitin-proteasome system postsynaptically regulates glutamatergic synaptic function. Mol Cell Neurosci 2007;35:64-75.
13. Gadadhar S, Bodakuntla S, Natarajan K, et al. The tubulin code at a glance. J Cell Sci 2017;130:1347-53.
14. Bodakuntla S, Jijumon AS, Villablanca C, et al. Microtubule-Associated Proteins: Structuring the Cytoskeleton. Trends Cell Biol 2019;29:804-19.
15. Etienne-Manneville S. From signaling pathways to microtubule dynamics: the key players. Curr Opin Cell Biol 2010;22:104-11.
16. Zhang YF, Xiong TQ, Tan BH, et al. Pilocarpine-induced epilepsy is associated with actin cytoskeleton reorganization in the mossy fiber-CA3 synapses. Epilepsy Res 2014;108:379-89.
17. Tang L, Lu Y, Zheng W, et al. Overexpression of MAP-2 via formation of microtubules plays an important role in the sprouting of mossy fibers in epileptic rats. J Mol Neurosci 2014;53:103-8.
18. Xi ZQ, Wang XF, Shu XF, et al. Is intractable epilepsy a tauopathy? Med Hypotheses 2011;76:897-900.
19. Machado RA, Benjumea-Cuartas V, Zapata Berruecos JF, et al. Reelin, tau phosphorylation and psychiatric complications in patients with hippocampal sclerosis and structural abnormalities in temporal lobe epilepsy. Epilepsy Behav 2019;96:192-9.
20. Huang ZL, Zhou Y, Xiao B, et al. Proteomic screening of postsynaptic density proteins related with temporal lobe epilepsy. Zhonghua Yi Xue Za Zhi 2008;88:3205-9.
21. André V, Ferrandon A, Marescaux C, et al. The lesional and epileptogenic consequences of lithium-pilocarpine-induced status epilepticus are affected by previous exposure to isolated seizures: effects of amygdala kindling and maximal electroshocks. Neuroscience 2000;99:469-81.
22. Wu Q, Li Y, Shu Y, et al. NDEL1 was decreased in the CA3 region but increased in the hippocampal blood vessel network during the spontaneous seizure period after pilocarpine-induced status epilepticus. Neuroscience 2014;268:276-83.
23. Furtado MA, Castro OW, Del Vecchio F, et al. Study of spontaneous recurrent seizures and morphological alterations after status epilepticus induced by intrahippocampal injection of pilocarpine. Epilepsy Behav 2011;20:257-66.
24. Curia G, Longo D, Biagini G, et al. The pilocarpine model of temporal lobe epilepsy. J Neurosci Methods 2008;172:143-57.
25. Liu S, Shen Y, Shultz SR, et al. Accelerated kindling epileptogenesis in Tg4510 tau transgenic mice, but not in tau knockout mice. Epilepsia 2017;58:e136-e141.
26. Jones NC, Nguyen T, Corcoran NM, et al. Targeting hyperphosphorylated tau with sodium selenate suppresses seizures in rodent models. Neurobiol Dis 2012;45:897-901.
27. Liu SJ, Zheng P, Wright DK, et al. Sodium selenate retards epileptogenesis in acquired epilepsy models reversing changes in protein phosphatase 2A and hyperphosphorylated tau. Brain 2016;139:1919-38.
28. Carletti F, Sardo P, Gambino G, et al. Hippocampal Hyperexcitability is Modulated by Microtubule-Active Agent: Evidence from In Vivo and In Vitro Epilepsy Models in the Rat. Front Cell Neurosci 2016;10:29.
29. White D, Honore S, Hubert F. Exploring the effect of end-binding proteins and microtubule targeting chemotherapy drugs on microtubule dynamic instability. J Theor Biol 2017;429:18-34.
30. Bayley PM, Schilstra MJ, Martin SR. A simple formulation of microtubule dynamics: quantitative implications of the dynamic instability of microtubule populations in vivo and in vitro. J Cell Sci. 1989;93:241-54.
31. Kim SK, Cho SM, Kim H, et al. The colchicine derivative CT20126 shows a novel microtubule-modulating activity with apoptosis. Exp Mol Med 2013;45:e19.
32. Choi MC, Chung PJ, Song C, et al. Paclitaxel suppresses Tau-mediated microtubule bundling in a concentration-dependent manner. Biochim Biophys Acta Gen Subj 2017;1861:3456-63.
33. Kilkenny C, Browne WJ, Cuthill IC, et al. Improving bioscience research reporting: the ARRIVE guidelines for reporting animal research. PLoS Biol 2010;8:e1000412.
34. Feng L, Li AP, Wang MP, et al. Plasticity at axon initial segment of hippocampal CA3 neurons in rat after status epilepticus induced by lithium-pilocarpine. Acta Neurochir (Wien) 2013;155:2373-80; discussion 2380.
35. Liu TT, Li Y, Shu Y, et al. Ephrinb3 modulates hippocampal neurogenesis and the reelin signaling pathway in a pilocarpine induced model of epilepsy. Int J Mol Med 2018;41:3457-67.
36. Racine R, Okujava V, Chipashvili S. Modification of seizure activity by electrical stimulation. 3. Mechanisms. Electroencephalogr Clin Neurophysiol. 1972;32:295-9.
37. Shu Y, Xiao B, Wu Q, et al. The Ephrin-A5/EphA4 Interaction Modulates Neurogenesis and Angiogenesis

by the p-Akt and p-ERK Pathways in a Mouse Model of TLE. Mol Neurobiol 2016;53:561-76.
38. Wyneken U, Smalla KH, Marengo JJ, et al. Kainate-induced seizures alter protein composition and N-methyl-D-aspartate receptor function of rat forebrain postsynaptic densities. Neuroscience 2001;102:65-74.
39. Yun-Hong Y, Chih-Fan C, Chia-Wei C, et al. A study of the spatial protein organization of the postsynaptic density isolated from porcine cerebral cortex and cerebellum. Mol Cell Proteomics 2011;10:M110 007138.
40. Schafer DP, Bansal R, Hedstrom KL, et al. Does paranode formation and maintenance require partitioning of neurofascin 155 into lipid rafts? J Neurosci 2004;24:3176-85.
41. Alsharafi WA, Bi FF, Hu YQ, et al. Effect of Khat on apoptosis and related gene Smac/DIABLO expression in the cerebral cortex of rats following transient focal ischemia. Environ Toxicol Pharmacol 2015;39:424-32.
42. Parajuli LK, Nakajima C, Kulik A, et al. Quantitative regional and ultrastructural localization of the Ca(v)2.3 subunit of R-type calcium channel in mouse brain. J Neurosci 2012;32:13555-67.
43. Paxinos G, Watson C. The rat brain in stereotaxic coordinates, 4th Edition. San Diego: Academic Press, 1998.
44. Goffin K, Nissinen J, Van Laere K, et al. Cyclicity of spontaneous recurrent seizures in pilocarpine model of temporal lobe epilepsy in rat. Exp Neurol 2007;205:501-5.
45. Arida RM, Scorza FA, Peres CA, et al. The course of untreated seizures in the pilocarpine model of epilepsy. Epilepsy Res. 1999;34:99-107.
46. Scholl EA, Dudek FE, Ekstrand JJ. Neuronal degeneration is observed in multiple regions outside the hippocampus after lithium pilocarpine-induced status epilepticus in the immature rat. Neuroscience 2013;252:45-59.
47. Sankar R, Rho JM. Do seizures affect the developing brain? Lessons from the laboratory. J Child Neurol 2007;22:21S-9S.
48. Deshpande LS, Lou JK, Mian A, et al. In vitro status epilepticus but not spontaneous recurrent seizures cause cell death in cultured hippocampal neurons. Epilepsy Res 2007;75:171-9.
49. Godale CM, Danzer SC. Signaling Pathways and Cellular Mechanisms Regulating Mossy Fiber Sprouting in the Development of Epilepsy. Front Neurol 2018;9:298.
50. Bates D, Eastman A. Microtubule destabilising agents: far more than just antimitotic anticancer drugs. Br J Clin Pharmacol 2017;83:255-68.
51. Walikonis RS, Jensen ON, Mann M, et al. Identification of proteins in the postsynaptic density fraction by mass spectrometry. J Neurosci 2000;20:4069-80.
52. Merriam EB, Millette M, Lumbard DC, et al. Synaptic regulation of microtubule dynamics in dendritic spines by calcium, F-actin, and drebrin. J Neurosci 2013;33:16471-82.
53. Yang JW, Czech T, Felizardo M, et al. Aberrant expression of cytoskeleton proteins in hippocampus from patients with mesial temporal lobe epilepsy. Amino Acids 2006;30:477-93.
54. do Nascimento AL, Dos Santos NF, Campos Pelagio F, et al. Neuronal degeneration and gliosis time-course in the mouse hippocampal formation after pilocarpine-induced status epilepticus. Brain Res 2012;1470:98-110.
55. Zhu BK, Wang P, Zhang XD, et al. Activation of Jun N-terminal kinase is a mediator of vincristine-induced apoptosis of melanoma cells. Anticancer Drugs 2008;19:189-200.
56. Gorter JA, Goncalves Pereira PM, van Vliet EA, et al. Neuronal cell death in a rat model for mesial temporal lobe epilepsy is induced by the initial status epilepticus and not by later repeated spontaneous seizures. Epilepsia 2003;44:647-58.
57. Represa A, Pollard H, Moreau J, et al. Mossy fiber sprouting in epileptic rats is associated with a transient increased expression of alpha-tubulin. Neurosci Lett. 1993;156:149-52.
58. Sutula TP, Dudek FE. Unmasking recurrent excitation generated by mossy fiber sprouting in the epileptic dentate gyrus: an emergent property of a complex system. Prog Brain Res 2007;163:541-63.
59. Walker MC. Pathophysiology of status epilepticus. Neurosci Lett 2018;667:84-91.
60. Wei J, Zhang M, Zhu Y, et al. Ca(2+)-calmodulin signalling pathway up-regulates GABA synaptic transmission through cytoskeleton-mediated mechanisms. Neuroscience 2004;127:637-47.
61. Lynch MA. Long-term potentiation and memory. Physiol Rev 2004;84:87-136.
62. Banan A, Zhang LJ, Farhadi A, et al. Critical role of the atypical {lambda} isoform of protein kinase C (PKC-{lambda}) in oxidant-induced disruption of the microtubule cytoskeleton and barrier function of intestinal epithelium. J Pharmacol Exp Ther 2005;312:458-71.
63. Puttachary S, Sharma S, Stark S, et al. Seizure-induced oxidative stress in temporal lobe epilepsy. Biomed Res Int 2015;2015:745613.

64. Mota SI, Ferreira IL, Pereira C, et al. Amyloid-beta peptide 1-42 causes microtubule deregulation through N-methyl-D-aspartate receptors in mature hippocampal cultures. Curr Alzheimer Res 2012;9:844-56.
65. Wyneken U, Marengo JJ, Villanueva S, et al. Epilepsy-induced changes in signaling systems of human and rat postsynaptic densities. Epilepsia 2003;44:243-6.
66. Stamboulian-Platel S, Legendre A, Chabrol T, et al. Activation of GABAA receptors controls mesiotemporal lobe epilepsy despite changes in chloride transporters expression: In vivo and in silico approach. Exp Neurol 2016;284:11-28.
67. Mattson MP. Effects of microtubule stabilization and destabilization on tau immunoreactivity in cultured hippocampal neurons. Brain Res 1992;582:107-18.
68. Michaelis ML, Ansar S, Chen Y, et al. {beta}-Amyloid-induced neurodegeneration and protection by structurally diverse microtubule-stabilizing agents. J Pharmacol Exp Ther 2005;312:659-68.
69. O'Sullivan D, Miller JH, Northcote PT, et al. Microtubule-stabilizing agents delay the onset of EAE through inhibition of migration. Immunol Cell Biol 2013;91:583-92.
70. Hoskison MM, Shuttleworth CW. Microtubule disruption, not calpain-dependent loss of MAP2, contributes to enduring NMDA-induced dendritic dysfunction in acute hippocampal slices. Exp Neurol 2006;202:302-12.

Cite this article as: Wu X, Zhou Y, Huang Z, Cai M, Shu Y, Zeng C, Feng L, Xiao B, Zhan Q. The study of microtubule dynamics and stability at the postsynaptic density in a rat pilocarpine model of temporal lobe epilepsy. Ann Transl Med 2020;8(14):863. doi: 10.21037/atm-19-4636

